

## Development of a Photoactivatable Protein Phosphatase-1-Disrupting Peptide

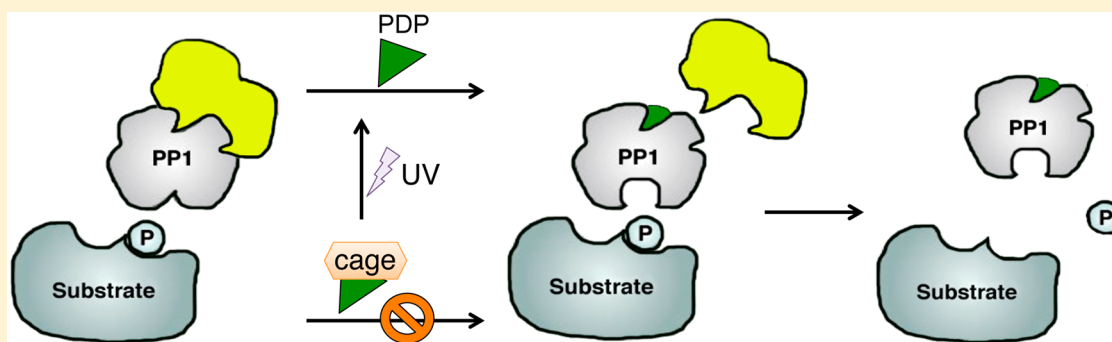
Malgorzata Trebacz,<sup>†,‡,§,⊥</sup> Yansong Wang,<sup>§,⊥</sup> Leslie Makotta,<sup>§</sup> Lars Henschke,<sup>§</sup> and Maja Köhn<sup>\*,†,‡,§,⊥</sup>

<sup>†</sup>Faculty of Biology, Institute of Biology III, University of Freiburg, Schänzlestraße 18, 79104 Freiburg, Germany

<sup>‡</sup>Signalling Research Centres BIOS and CIBSS, University of Freiburg, 79104 Freiburg, Germany

<sup>§</sup>European Molecular Biology Laboratory, Genome Biology Unit, Meyerhofstraße 1, 69117 Heidelberg, Germany

### Supporting Information



**ABSTRACT:** We describe here the development of a photoreleasable version of a protein phosphatase-1 (PP1)-disrupting peptide (PDP-*Nal*) that triggers protein phosphatase-1 activity. PDP-*Nal* is a 23 mer that binds to PP1 through several interactions. It was photocaged on a tyrosine residue, which required the exchange of phenylalanine in PDP-*Nal* to tyrosine in order to disrupt the most important binding interface. This PDP-*caged* can be light-controlled in live cells.

Protein phosphatase-1 (PP1) is a ubiquitously expressed phospho-serine/threonine-specific phosphatase that is involved in numerous signaling processes like cell division or insulin secretion, making it a potential therapeutic target in diseases such as cancer or diabetes.<sup>1,2</sup> PP1 counteracts more than 100 kinases through regulation by more than 200 regulatory interactors of protein phosphatase one (RIPPOs), with which PP1 forms holoenzymes.<sup>3,4</sup> The most common motif, which is involved in the binding of RIPPOs, is the so-called RVxF-type motif (single amino acid abbreviation code, x = any amino acid except proline). PP1-disrupting peptides (PDPs) are currently the only selective modulators targeting the PP1 catalytic subunit, and they contain the sequence RVTF as the RVxF-type motif.<sup>5</sup> They disrupt a subset of PP1 holoenzymes, which results in the rapid dephosphorylation of nearby substrates. PDPs were designed based on the sequence of the RIPPO nuclear inhibitor of PP1 (NIPPI).<sup>5</sup> They are proteolytically stable in cellular assays<sup>5,6</sup> due to the incorporation of an unnatural amino acid in the sequence and because of amidation and acetylation at the C- and N-terminus, respectively.<sup>5,6</sup> The polybasic sequence at the N-terminus of PDPs was optimized to render these peptides cell-permeable.<sup>5</sup> Optimization of the sequence has led to the creation of PDP-*Nal* (for the sequence see Table 1), which exhibits improved stability and potency.<sup>6</sup> PDPs have been used to study PP1 substrates in the mitogen-activated protein kinase (MAPK) pathway,<sup>6</sup> PP1's role in calcium release,<sup>7</sup> and for

activation of PP1 to treat arrhythmia and heart failure.<sup>8,9</sup> Since this rather general release of PP1 activity is expected to impact several substrates and pathways, in order to study specific roles of PP1, there is a need for a more controlled modulation of its activity. Photocleavable groups (cages) can be used to block the interaction of a ligand to a protein. Irradiation with light releases the cage, activating the ligand that can then bind to a protein and modulate its activity. Thus, photocaging allows for temporal control by light irradiation of the ligand binding to a protein.<sup>10–12</sup> Nitrobenzyl derivatives are the most commonly applied photolabile protecting groups. They are simple to synthesize, relatively stable, and easy to mimic with a benzyl group to screen for the optimal position of a cage in a peptide. They can be cleaved with UV light at 365 nm. Coumarin derivatives allow irradiation at longer wavelengths. Coumarins are also relatively simple to synthesize and release the substrate rapidly after visible-light and two-photon irradiation. Moreover, their fluorescent properties can be used for tracking molecules inside the cells. Yet, handling them under ambient light can cause partial uncaging. Both coumarin-based and nitrobenzyl-based caging groups have been applied in cells.<sup>11–13</sup> Cyanine-based caging groups exhibit a similar

**Special Issue:** Modern Peptide and Protein Chemistry

**Received:** September 19, 2019

**Published:** December 16, 2019

**Table 1.** Activity of (Nitro-) Benzylated PDP-*Nal*-Derived Peptides<sup>a</sup>

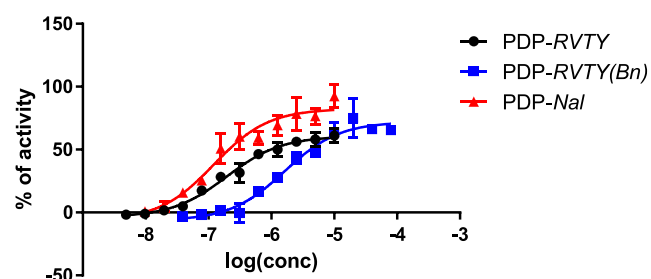
peptide	sequence	EC <sub>50</sub> [ $\mu$ M]
PDP- <i>Nal</i>	RRKRPKRKRKNARVTF <i>Nal</i> /EAAEII	0.144 $\pm$ 0.040
PDP-RVTY	RRKRPKRKRKNARVTY <i>Nal</i> /EAAEII	0.194 $\pm$ 0.005
PDP-RVTY( <i>Bn</i> )	RRKRPKRKRKNARVTY( <b>Bn</b> ) <i>Nal</i> EAAEII	1.63 $\pm$ 0.04
PDP-caged	RRKRPKRKRKNARVTY( <b>Nb</b> ) <i>Nal</i> EAAEII	>1.00
PDP-RTTY	RRKRPKRKRKNARTTY <i>Nal</i> /EAAEII	7.59 $\pm$ 0.89
PDP-RT( <i>Bn</i> ) TY( <i>Bn</i> )	RRKRPKRKRKNART( <b>Bn</b> )TY( <b>Bn</b> ) <i>Nal</i> EAAEII	>2.30

<sup>a</sup>Amino acids crucial for the binding to the pocket of PP1 carried a benzyl group (Bn) on the hydroxyl group on the side chain of the amino acid in order to mimic the Nb cage. EC<sub>50</sub> values were determined by a dephosphorylation assay using recombinant PP1 and I2 with DiFMUP as a substrate. The RVxF motif is marked in bold, and changes are marked in red. Error for PDP-*Nal*, PDP-RVTY, PDP-RVTY(*Bn*): standard error of the mean of two independent triplicate measurements ( $n = 6$ ). Error for PDP-RTTY: standard deviation from the curve taken from one triplicate measurement ( $n = 3$ ). PDP-caged was measured in two independent triplicate measurements, PDP-RT(*Bn*)TY(*Bn*), in one triplicate measurement.

fluorescent character and are uncaged with near-infrared light. However, the complexity and size of the molecules can be a disadvantage.<sup>11,13</sup> Applications of the caging approach for peptides have been described previously. For example, nitrobenzyl-derived cages have been used to study kinase activity<sup>14,15</sup> and have been applied in hydrogels for caging RGDS peptides in order to create a nonadhesive surface with patches containing the uncaged RGDS peptide where cells can bind,<sup>16</sup> and for making a cell-penetrating peptide light-sensitive in order to enhance drug delivery to tumor cells.<sup>17</sup> Here, we report the development of a caged PDP for photocontrol of PP1 activity. Due to the fact that most studies with caged peptides were so far done with the nitrobenzyl (Nb) cage or a derivative,<sup>14–17</sup> and because the Nb group is relatively stable under ambient light allowing simple handling, we focused here on the Nb group as a cage.

PDPs are 23 mer peptides that have several interaction points with PP1,<sup>5</sup> which could be problematic when designing a caged molecule. A single cage would only interrupt one area of interaction, and more cages might be required to efficiently disrupt the interaction between these long peptides and PP1. However, the exchange of the RVTF sequence in the PDPs to RATA (this version is called “PDPm”) caused the PDPs to not bind PP1 anymore,<sup>5</sup> which provided the possibility that introducing one cage within this motif could be sufficient to disrupt the interaction PP1 with the PDP. Previously, serine was caged with a 4,5-dimethoxy-2-nitrobenzyl group (DMNb) and applied successfully in photorelease studies with peptides.<sup>14,15</sup> Therefore, Fmoc-Ser(DMNb)-OH was synthesized according to literature procedures<sup>15</sup> and incorporated into PDP-*Nal*, replacing the threonine of the RVTF sequence (PDP-RVS(DMNb)F). Then, the efficacy of PDP-RVS(DMNb)F to disrupt the PP1:inhibitor 2 (I2) holoenzyme was tested, which would lead to free PP1 catalytic subunit that dephosphorylates an unnatural substrate (6,8-difluoro-4-methylumbelliferyl phosphate, DiFMUP) measured by a fluorescence change.<sup>5,6</sup> However, this modification did not significantly lower the potency of the PDP (data not shown), which was likely due to the fact that the caged serine was placed at the flexible position of the RVxF-type motif.

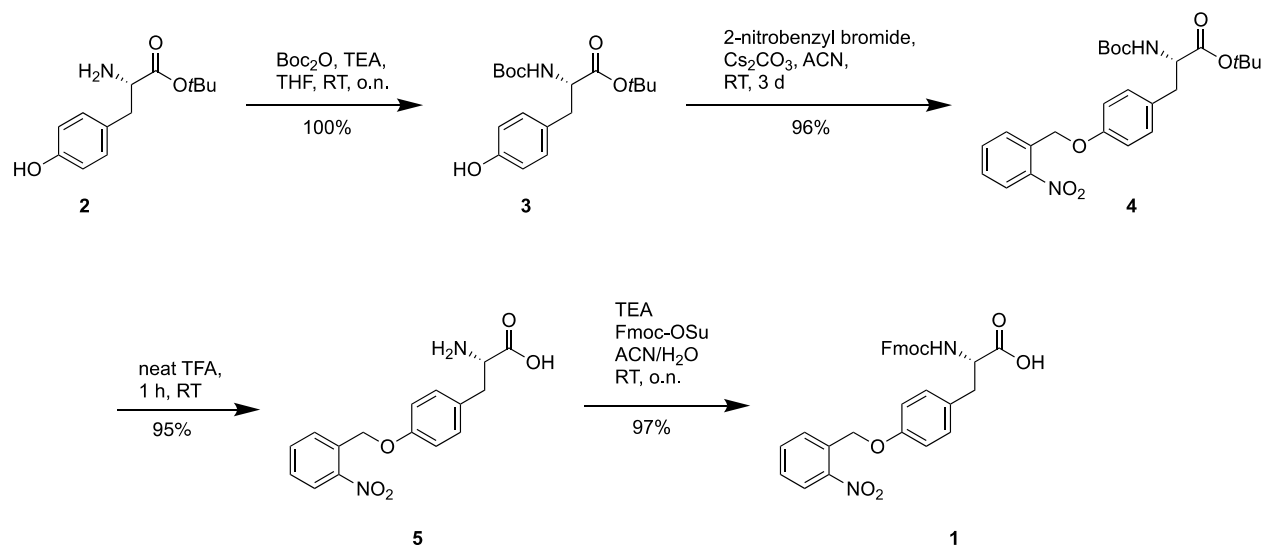
Due to the known importance of valine and phenylalanine of the RVTF sequence for binding of PDPs to PP1 as shown by the inactive RATA version,<sup>5</sup> we next interrogated if caging of F and/or V would result in loss of potency. As caging of valine and phenylalanine would only be possible upon the introduction of a hydroxyl group, they were replaced by the structurally similar threonine and tyrosine. Because testing of different positions for the cage was required, for synthetic ease, we used commercially available benzylated tyrosine and threonine (Table 1), mimicking the Nb group. When monitoring the potency of PDP-*Nal* and PDP-RVTY peptide, only a slight change was observed, with the EC<sub>50</sub> changing from 144 to 194 nM, respectively. However, replacing valine with threonine in the PDP-RVTY peptide to PDP-RTTY led to an about 40 times higher EC<sub>50</sub>, which excluded this change from further use. The benzylated PDP-RVTY(*Bn*) peptide was more than 8 times less potent than the nonbenzylated PDP-RVTY (Table 1, Figure 1). This was judged to be a large enough difference to develop the caged PDP-RVTY(*Nb*) peptide.



**Figure 1.** Difference of the kinetics of PDP-*Nal* (red triangles), PDP-RVTY (black dots), and PDP-RVTY(*Bn*) (blue squares). The area between the curves illustrates the activity difference between the peptides. The dephosphorylation assay was carried out with recombinant PP1 and I2 using DiFMUP as a substrate. The error is the standard deviation of two independent triplicate measurements ( $n = 6$ ).

First, the building block Fmoc-Tyr(Nb)-OH **1** (Scheme 1) needed to be synthesized. The synthesis of **1** had been described previously.<sup>18–20</sup> We adapted the synthesis procedure, starting with Tyr-*t*Bu **2** for synthetic simplicity and reported good yields,<sup>20</sup> but optimized conditions for scaling up to several grams (Scheme 1). First, the free amine was protected using Boc-anhydride. For the nitrobenzylation step, compound **3** was reacted with nitrobenzyl bromide and Cs<sub>2</sub>CO<sub>3</sub> in acetonitrile (ACN), which gave compound **4** in an excellent yield of 96% at the gram scale. Deprotection of the *t*Bu-ester and the Boc-group was achieved with neat TFA, and after subsequent protection of the amine using Fmoc-OSu, Fmoc-Tyr(Nb)-OH **1** was obtained in an almost quantitative yield (Scheme 1). This building block was then incorporated into the PDP using standard Fmoc solid-phase synthesis, resulting in the peptide PDP-RVTY(*Nb*), which we called PDP-caged (see the sequence in Table 1).

When testing PDP-caged in the activity assay, we noted large error bars at higher concentrations and varying results (data not shown). It is possible that this was due to uncaging during light exposure in the plate reader. Therefore, we were not able to determine an exact EC<sub>50</sub>. Nevertheless, we assumed that this peptide would behave similarly to the PDP-RVTY(*Bn*) peptide,

Scheme 1. Synthesis of Fmoc-Tyr(Nb)-OH **1**<sup>a</sup>

<sup>a</sup>ACN: acetonitrile. Boc-ON: 2-(*tert*-butoxycarbonyloxyimino)-2-phenylacetoneitrile. d: day(s). DMF: *N,N*-dimethyl formamide. Fmoc-OSu: 9-fluorenylmethyl-succinimidyl carbonate. o.n.: overnight. RT: room temperature. TEA: triethylamine. *t*Bu: *tert*-butyl. TFA: trifluoroacetic acid. THF: tetrahydrofuran.

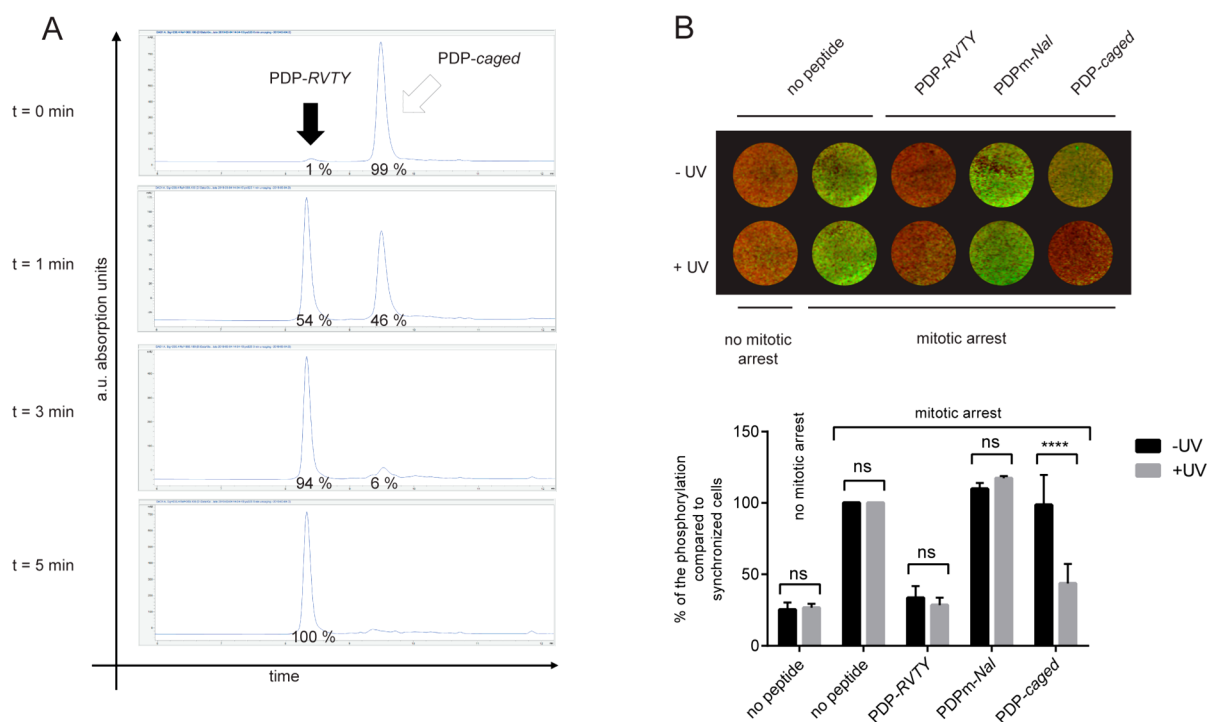


**Figure 2.** Uncaging experiments of PDP-caged *in vitro* and *in cells*. (A) *In vitro* photocleavage of PDP-caged. HPLC traces for the peptide exposed to  $\lambda = 365$  nm light for 1, 3, or 5 min are shown. (B) Dephosphorylation of H3pT3 after treatment with 40  $\mu$ M PDPs, with or without UV irradiation (+UV/-UV). U2OS cells were synchronized in mitotic arrest. *In-cell* Western analysis was used to detect phosphorylation levels. An inactive mutant of PDP-Nal containing a RATA sequence instead of RVTF was used as a negative control (PDPm-Nal). Red: Total histone 3. Green: H3pT3. The respective signal intensity of H3pT3/total histone 3 was compared to “mitotic arrest, no peptide”. For quantification, three independent experiments were used (see Supporting Figure S2 for the other two replicates). Results were analyzed with GraphPad Prism 6. Statistical analysis is based on two-way ANOVA and Bonferroni multiple comparison test. (<sup>ns</sup>*P* > 0.05, <sup>\*\*\*\*</sup>*P* < 0.0001; *n* = 3).

and would disrupt the PP1:I2 interaction with a lesser potency than PDP-RVTY, and therefore carried on with PDP-caged.

Next, we characterized the stability of PDP-caged. After 24 h of exposure under ambient light as well as in the dark, we did not notice any degradation (Supporting Figure S1). This confirms that the nitrobenzyl group is cleaved only with UV

light, which makes it easier to handle PDP-caged under ambient light. We then tested if PDP-caged could be uncaged *in vitro*. To this end, the peptide was exposed to light at 365 nm for a certain amount of time, and the product formation to PDP-RVTY was monitored using HPLC. After 3 min, the product had formed to 94%, and after 5 min, the caged peptide

was visible only in a negligible amount (Figure 2A). Finally, we asked whether a difference in activity of PDP-caged and PDP-RVTY could be detected in a cell assay and whether the activity of PDP-caged could be released through uncaging. To address this, we adapted the previously established dephosphorylation of the phosphorylated threonine 3 on histone H3 (H3pT3) upon PDP treatment<sup>5,6</sup> to uncaging conditions. H3pT3 is a substrate of PP1 that is phosphorylated at the beginning of mitosis. The PP1:Repoman holoenzyme dephosphorylates H3pT3 at the end of mitosis, enabling mitotic exit.<sup>21,22</sup> PDP3 and PDP-Nal treatment both led to the dephosphorylation of H3pT3 during mitotic arrest.<sup>5,6</sup> Here, U2OS cells were synchronized in mitotic arrest and then treated with PDP-RVTY (positive control), PDPm-Nal (negative control containing the RATA sequence instead of RVTF),<sup>6</sup> and PDP-caged, or left untreated (Figure 2B). Treatment occurred with 40  $\mu$ M final concentration of the peptides for 15 min; then the cells were washed and afterward irradiated for 5 min with UV light ( $\lambda = 365$  nm). Following another 10 min of incubation, the cells were fixed and stained with antibodies against total histone H3 and H3pT3. For the experimental read-out, we used the so-called *in-cell* Western method, which is similar to immunocytochemistry. The analysis showed that phosphorylation of H3pT3 was enhanced in arrested cells. As expected, treatment with PDP-RVTY led to a reduction of the phosphorylation level, whereas the addition of the negative control PDPm-Nal did not reduce the phosphorylation on H3pT3. Importantly, PDP-caged treatment only reduced the H3pT3 phosphorylation level after irradiation with UV light to a similar level as the positive control PDP-RVTY did. All other conditions were inert to UV light treatment, showing that the UV light-dependent activation is specific to PDP-caged. Thus, PDP-RVTY shows a similar activity like PDP-Nal<sup>6</sup> in this cellular assay, and the activity of PDP-caged can be controlled using UV light irradiation in live cells.

In summary, we developed here PDP-caged as a light-controllable modulator of PP1 activity in live cells. While PDP-caged contains 23 amino acids, of which several interact with PP1,<sup>5</sup> targeting phenylalanine of the RVxF-type binding motif for replacement with a caged tyrosine was sufficient to disrupt the interaction between the PDP and PP1. PDP-caged allows releasing PP1 activity in a timely, precise manner through UV light irradiation at specific time points. A limitation of the Nb group when used in biological systems is that UV light irradiation is cytotoxic and has a limited penetration ability through tissue.<sup>11,12</sup> In the proof-of-concept settings used here, the wavelength (365 nm) is close to visible light, and the irradiation time is short. Therefore, it is not expected that the cytotoxicity would cause problems in these settings, as seen in the controls. For more complex applications, however, red-shifted derivatives of Nb or Coumarin and possibly two-photon excitation might have to be applied.<sup>11,12</sup> We expect that this compound will prove to be a useful tool in time-sensitive studies of PP1 activity in cellular processes, such as in different stages of mitosis<sup>23,24</sup> and in the regulation of calcium homeostasis in the heart.<sup>25</sup>

## EXPERIMENTAL SECTION

**General Information.** Tyr(OtBu) was bought from Bachem, Switzerland. DIPEA (*N,N*-diisopropylethylamine), Fmoc-Thr(Bn)-OH, and Fmoc-Tyr(Bn)-OH were purchased from ABCR. HOBt (*N*-hydroxybenzotriazole) was bought from MOLEKULA. Triisopropylsilane and cesium carbonate were from Alfa Aesar. Dithiothreitol

(DTT), imidazole, MnCl<sub>2</sub>, bovine serum albumin (BSA), pyridine, di-*tert*-butyl dicarbonate (Boc<sub>2</sub>O), triethylamine (TEA), 2-nitrobenzyl bromide, sodium hydroxide, acetic anhydride (Ac<sub>2</sub>O), and chloroform-*d* were from Sigma. Dioxane, DCM (dichloromethane), Cy (cyclohexane), EA (ethyl acetate), methanol and sodium sulfate, TFA (trifluoroacetic acid), piperidine, and ACN (acetonitrile) were from Roth. Other Fmoc-amino acids, 9-fluorenylmethyl-succinimidyl carbonate (Fmoc-OSu), and HBTU (*O*-(benzotriazol-1-yl)-*N,N,N',N'*-tetramethyluronium hexafluorophosphate) were from Novabiochem. Acetic anhydride and DMF (*N,N*-dimethylformamide) were from Merck Millipore. DiFMUP (6,8-difluoro-4-methylumbelliferyl phosphate) was purchased from Life Technologies.

**<sup>1</sup>H and <sup>13</sup>C Nuclear Magnetic Resonance.** All spectra were recorded on a 400 MHz Bruker Avance DPX and a 500 MHz Bruker DRX. For LC/MS analysis and HPLC purification, LC/MS analysis and HPLC peptide purifications were carried out on a Shimadzu high-performance liquid chromatograph coupled with a mass spectrometer using a UV-vis Photodiode array detector, SPD-M20A Prominence, unless otherwise noted. ESI-MS of PDP-caged was performed on an Agilent Technologies 1260 Infinity I/II coupled to 6120 Quadrupole LC/MS. The solvent used for all analytical and semipreparative runs was a mixture of H<sub>2</sub>O containing 0.05% TFA and ACN containing 0.05% TFA. RP-HPLC analytical runs were realized with a Macherey Nagel C18 EC 250/4.0 NUCLEODUR 100–5 C18 ec column and a pump rate of 1.5 mL/min. RP-HPLC semipreparative separations were performed with a Macherey Nagel C18 VP 250/10 NUCLEODUR 110–5 C18 ec column in gradients ranging between 31 and 43% of ACN over 30 min using a flow rate of 5 mL/min. Semipreparative HPLC of PDP-RVTY was run on an Agilent Technologies 1260 I/II Infinity system using a gradient of ACN 10–70% over 30 min. Flash chromatography purifications were performed using silica gel 60 (Roth), grain size 0.04–0.063 mm, 230–400 mesh ASTM. The mass of all peptides was recorded on MALDI-TOF (matrix-assisted laser desorption/ionization coupled with time of flight) with the MALDI micro MX mass spectrometer (Waters, Manchester, U.K.) equipped with a reflection analyzer used in positive ion mode with activated delayed mode. The matrix was prepared by weighing out 10–20 mg of  $\alpha$ -cyano-4-hydroxycinnamic acid (CHCA) in an Eppendorf tube and then adding 1.0 mL of 50:50 H<sub>2</sub>O/ACN with a 0.1% TFA final concentration.

**Peptide Synthesis.** All peptides were synthesized using solid-phase peptide synthesis on the automated liquid handling system, Syro I from MultisynTech, using the Fmoc protection strategy.<sup>5,6</sup> Peptide elongation was carried out on the Rink Amide Resin, using HBTU/HOBt double coupling (5 equiv of amino acid, 5 equiv of HBTU, 2 equiv of HOBt and 10 equiv of DIPEA in DMF) for 40 min with 15 s vortexing every 4 min. The Fmoc deprotection was carried out using 20% piperidine. The capping step was done twice after every double coupling with 10% Ac<sub>2</sub>O/pyridine mixture for 5 min with 10 s vortexing every minute. The cleavage cocktail contained 95% TFA, 2.5% TIS, and 2.5% water. After cleavage the peptides were precipitated in ice-cold diethyl ether, HPLC-purified, and analyzed by MALDI (Supporting Table S1). The synthesis of PDP-Nal was described before.<sup>5</sup>

**Preparation of (2S)-2-*tert*-Butyl Carbamate-3-(4-hydroxyphenyl)propanoic Acid *tert*-Butyl Ester: Boc-Tyr-OtBu 3.** Tyr-OtBu 2 (2.00 g, 8.42 mmol), Boc<sub>2</sub>O (1.84 g, 8.42 mmol), and TEA (114  $\mu$ L, 0.84 mmol) were stirred in 100 mL of THF at RT overnight. THF was removed *in vacuo*. The mixture was dissolved in EA, washed three times with water, and dried over sodium sulfate. It was purified using the gradient 20%–40% EA in Cy. Yield: 2.84 g (8.42 mmol), 100%, white solid. <sup>1</sup>H NMR (400 MHz, DMSO-*d*<sub>6</sub>):  $\delta$  9.21 (s, 1H),  $\delta$  7.09 (d, *J* = 7.92 Hz, 1H),  $\delta$  7.00 (d, *J* = 8.36 Hz, 2H),  $\delta$  6.65 (d, *J* = 8.32 Hz, 2H),  $\delta$  3.91 (dt, *J* = 6.22, 8.38 Hz, 1H),  $\delta$  2.83–2.66 (m, 2H),  $\delta$  1.36–1.32 (m, 18H). These data are in agreement with a reference.<sup>20</sup>

**Preparation of (2S)-2-*tert*-Butyl Carbamate-3-{4-[2-nitrophenyl]methoxy}phenyl}propanoic Acid *tert*-Butyl Ester: Boc-Tyr(Nb)-OtBu 4.** Boc-Tyr-OtBu 3 (2.76 g, 8.19 mmol), 2-nitrobenzyl bromide (1.77 g, 8.19 mmol), and Cs<sub>2</sub>CO<sub>3</sub> (2.93 g, 3.00 mmol) were dissolved in

ACN (30 mL). The reaction was stirred for 3 days at room temperature. The reaction mixture was filtered, the solvent was reduced *in vacuo*, and the compound was purified using flash chromatography (2% EA in Cy to 10% EA in Cy). Yield: 3.70 g (7.83 mmol), 96%, orange oil.  $R_f = 0.45$  (Cy/EA = 12/1).  $^1\text{H}$  NMR ( $\text{CDCl}_3$ , 400 MHz):  $\delta$  8.16 (d,  $J = 8.16$  Hz, 1H),  $\delta$  7.87 (d,  $J = 7.80$  Hz, 1H),  $\delta$  7.66 (t,  $J = 7.56$  Hz, 1H),  $\delta$  7.47 (t,  $J = 7.76$  Hz, 1H),  $\delta$  7.10 (d,  $J = 8.48$  Hz, 2H),  $\delta$  6.90 (d,  $J = 8.52$  Hz, 2H),  $\delta$  5.45 (s, 2H),  $\delta$  5.00 (d,  $J = 8.00$  Hz, 1H),  $\delta$  4.44–4.37 (m, 1H),  $\delta$  3.02–2.96 (m, 2H),  $\delta$  1.41 (s, 9H),  $\delta$  1.40 (s, 9H).  $^{13}\text{C}\{^1\text{H}\}$  NMR (125 MHz):  $\delta$  171.0,  $\delta$  157.0,  $\delta$  155.1,  $\delta$  146.9,  $\delta$  134.0,  $\delta$  130.7,  $\delta$  129.4,  $\delta$  128.5,  $\delta$  128.3,  $\delta$  125.0,  $\delta$  114.8,  $\delta$  82.0,  $\delta$  79.6,  $\delta$  66.8,  $\delta$  54.9,  $\delta$  37.6,  $\delta$  28.3,  $\delta$  28.0. MS  $m/z$ :  $[\text{M} + \text{Na}]^+$  calcd for  $\text{C}_{25}\text{H}_{32}\text{N}_2\text{O}_7$ , 495.21; found  $[\text{M} + \text{Na}]^+$ , 495.20. These data are in agreement with a reference.<sup>20</sup>

**Preparation of (2S)-2-Amino-3-[4-[2-nitrophenyl)methoxy]phenyl]propanoic Acid: Tyr(Nb)-OH 5.** Boc-Tyr(Nb)-OtBu 4 (3.70 g, 7.83 mmol) was dissolved in TFA (75 mL). The reaction was stirred for 1 h at room temperature and was monitored by thin-layer chromatography (10% EA in Cy). TFA was coevaporated with toluene *in vacuo*, and the compound was dried under a high vacuum. Yield: 2.35 g (7.43 mmol), 95%, orange-brown solid. The product was used further without purification and analytical data collection.<sup>20</sup>

**Preparation of (2S)-2-Fluorenylmethylloxycarbamate-3-[4-[2-nitrophenyl)methoxy]phenyl]propanoic Acid: Fmoc-Tyr(Nb)-OH 1.** Tyr(Nb)-OH 5 (7.43 mmol), Fmoc-OSu (3.01 g, 8.92 mmol), and  $\text{Et}_3\text{N}$  (2.55 mL, 18.6 mmol) were dissolved in  $\text{ACN}/\text{H}_2\text{O}$  (7:4, 33 mL), stirred overnight at RT, dried *in vacuo*, and purified using flash chromatography (DCM only, then DCM/MeOH = 12/1 and 9/1). Yield: 3.98 g (7.39 mmol), 97%, orange-brown solid.  $R_f = 0.47$ .  $^1\text{H}$  NMR ( $\text{CDCl}_3$ , 400 MHz)  $\delta$  8.16 (d,  $J = 8.1$  Hz, 1H),  $\delta$  7.86 (d,  $J = 7.8$  Hz, 1H),  $\delta$  7.75 (d,  $J = 7.5$  Hz, 2H),  $\delta$  7.65 (t,  $J = 7.54$  Hz, 1H),  $\delta$  7.56–7.52 (m, 2H),  $\delta$  7.47 (t,  $J = 7.8$  Hz, 1H),  $\delta$  7.39 (t,  $J = 7.4$  Hz, 2H),  $\delta$  7.30 (t,  $J = 7.4$  Hz, 2H),  $\delta$  7.07 (d,  $J = 8.2$  Hz, 2H),  $\delta$  6.90 (d,  $J = 8.3$  Hz, 2H),  $\delta$  5.43 (s, 2H),  $\delta$  5.22 (d,  $J = 7.9$  Hz, 1H),  $\delta$  4.68–4.63 (m, 1H),  $\delta$  4.46 (dd,  $J = 10.4, 7.0$  Hz, 1H),  $\delta$  4.36 (dd,  $J = 10.3, 7.2$  Hz, 1H),  $\delta$  4.19 (t,  $J = 6.8$  Hz, 1H),  $\delta$  3.16 (dd,  $J = 14.3, 4.9$  Hz, 1H),  $\delta$  3.07 (dd,  $J = 13.9, 5.8$  Hz, 1H).  $^{13}\text{C}\{^1\text{H}\}$  NMR (100 MHz)  $\delta$  175.5,  $\delta$  157.4,  $\delta$  155.8,  $\delta$  146.9,  $\delta$  143.7,  $\delta$  143.7,  $\delta$  141.3,  $\delta$  134.0,  $\delta$  133.8,  $\delta$  130.6,  $\delta$  128.5,  $\delta$  128.3,  $\delta$  128.3,  $\delta$  127.8,  $\delta$  127.1,  $\delta$  125.0,  $\delta$  120.0,  $\delta$  115.1,  $\delta$  87.2,  $\delta$  67.0,  $\delta$  66.8,  $\delta$  54.6,  $\delta$  47.2,  $\delta$  36.9. MS  $m/z$ :  $[\text{M} + \text{Na}]^+$  calcd for  $\text{C}_{31}\text{H}_{26}\text{N}_2\text{O}_7$ , 561.16; found  $[\text{M} + \text{Na}]^+$ , 561.15. These data are in agreement with a reference.<sup>20</sup>

**Protein Expression and Purification.** Recombinant PP1 and I2 were obtained as described in Wang et al., 2019.<sup>6</sup>

**Activity Assay.**<sup>6</sup> Recombinant PP1 protein (25 pM final assaying concentration), I2 phosphatase inhibitor (1 nM final assaying concentration), and PDP at various concentrations were incubated in assay buffer (25 mM imidazole, 50 mM NaCl, BSA 0.1 mg/mL, 1 mM DTT, 0.3 mM  $\text{MnCl}_2$ , pH 7.4) for approximately 20 min at 25 °C, followed by the addition of DiFMUP to reach a final concentration of 135  $\mu\text{M}$  ( $K_m$  value). The dephosphorylation of DiFMUP to the fluorescent product was monitored for 40 min on a TECAN Infinite M1000 PRO fluorescence microplate reader with an excitation at 358 nm and emission at 452 nm. All experiments were performed two times in triplicates, with the exception of peptides PDP-RTTY and PDP-RT(Bn)TY(Bn), which were measured in one triplicate. After baseline normalization (assay in the absence of PDP), the reaction rates were plotted versus the log of the inhibitor concentrations, and the  $\text{EC}_{50}$  values were obtained by fitting the curves using the one-site competition model of GraphPad Prism (GraphPad Software, Version 6).

**In Vitro Uncaging Reaction and PDP-Caged Stability.** 100 Mm Pdp (10% DMSO in  $\text{H}_2\text{O}$ ) was exposed to UV light using the UVP Cross-Linker 365 nm (CL-1000L  $\lambda = 365$  nm) with the light dose of 120 mJ per  $\text{cm}^2$  or ambient light either for 3 min or for 24 h. The  $t = 0$  control sample was kept in the dark for the time of the experiment. Samples were acquired on the Agilent HPLC system using a 10–90% gradient of ACN in  $\text{H}_2\text{O}$ . Data were analyzed using the OpenLAB CDS Software (Agilent).

**Cell Line.**<sup>6</sup> U2OS human female osteosarcoma cells were cultured at 37 °C in a humidified incubator under an atmosphere of 5%  $\text{CO}_2$ . The cells were grown in Dulbecco's modified Eagle's medium (DMEM) containing 1 g/L glucose, 10% (v/v) fetal bovine serum (FBS), 1% (v/v) penicillin/streptomycin, and 2 mM L-glutamine.

**In-Cell Western Assay.**<sup>6</sup> Garnier bio-one CELLSTAR 12-well plates were coated with 0.1 mg/mL poly-D-lysine for 5 min, washed with PBS, and left to dry for 2 h. U2OS cells were plated in 1:100 dilution 1 day before starting the experiment. Culture media containing 2 mM thymidine was added and, after 24 h, exchanged to the media without thymidine for 2 h. Cells were treated with nocodazole for 15 h in the concentration of 100 ng/mL to allow the mitotic arrest. All peptides were diluted in the imaging buffer (115 mM NaCl, 1.2 mM  $\text{CaCl}_2$ , 1.2 mM  $\text{MgCl}_2$ , 1.2 mM  $\text{K}_2\text{HPO}_4$ , 20 mM HEPES, and 2 g/L D-glucose) containing 100 ng/mL nocodazole to reach the final concentration of 40  $\mu\text{M}$  and were added to the wells for 15 min. Cells were then washed with PBS and supplemented with fresh imaging buffer containing nocodazole. Five min uncaging was conducted using the UVP Cross-linker 365 nm (CL-1000L  $\lambda = 365$  nm) with a light dose of 120 mJ per  $\text{cm}^2$ . Plates were placed in the incubator for another 10 min to allow PP1 activation. Cells were fixed with ice-cold MeOH for 10 min, washed with PBS, and blocked for 1.5 h with Odyssey Blocking Buffer (PBS) (LI-COR). Primary antibodies against phosphorylated histone 3 on threonine 3 (H3pT3) (Millipore, cat. no. 07-424) and total histone 3 (Active Motif, cat. no. 39763) in dilution 1:500 were added and incubated for 2 h. Wells were washed with *in-cell* Western Washing Buffer (0.5% Triton-X in PBS) 3 times for 5 min. Secondary antibodies staining was performed using IRDye680RD Goat anti-Mouse IgG (H+L) (LI-COR, cat. no. 925-68070) and IRDye800CW Goat anti-Rabbit IgG (H+L) (LI-COR, cat. no. 925-32211) in the dilution of 1:1000 and incubated for 1 h. Wells were washed with the *in-cell* Western Washing Buffer (0.5% Triton-X in PBS) 3 times for 5 min. PBS was added, and plates were acquired on the LI-COR Odyssey CLX Imager. Data analysis was carried out using the software Image Studio Lite (LI-COR).

## ■ ASSOCIATED CONTENT

### 📄 Supporting Information

The Supporting Information is available free of charge at <https://pubs.acs.org/doi/10.1021/acs.joc.9b02548>.

NMR spectra and analytical data of compounds and peptides (PDF)

## ■ AUTHOR INFORMATION

### Corresponding Author

\*E-mail: [maja.koehn@bioss.uni-freiburg.de](mailto:maja.koehn@bioss.uni-freiburg.de).

### ORCID

Maja Köhn: 0000-0001-8142-3504

### Author Contributions

<sup>1</sup>M.T. and Y.W. contributed equally.

### Notes

The authors declare no competing financial interest.

## ■ ACKNOWLEDGMENTS

M.K. acknowledges financial support from the European Research Council through ERC starting grant no. 336567 and from the German Science Foundation (DFG) through the German Excellence Strategy (BIOS, EXC-294 and CIBSS, EXC-2189, Project ID 390939984). Gefördert durch die Deutsche Forschungsgemeinschaft (DFG) im Rahmen der Exzellenzstrategie des Bundes und der Länder, EXC 2189 (390939984).

## REFERENCES

- (1) Chatterjee, J.; Köhn, M. Targeting the untargetable: recent advances in the selective chemical modulation of protein phosphatase-1 activity. *Curr. Opin. Chem. Biol.* **2013**, *17*, 361–368.
- (2) Heroes, E.; Lesage, B.; Görnemann, J.; Beullens, M.; Van Meervelt, L.; Bollen, M. The PP1 binding code: a molecular-lego strategy that governs specificity. *FEBS J.* **2013**, *280*, 584–595.
- (3) Li, X.; Wilmanns, M.; Thornton, J.; Köhn, M. Elucidating human phosphatase-substrate networks. *Sci. Signaling* **2013**, *6*, rs10.
- (4) Wu, D.; De Wever, V.; Derua, R.; Winkler, C.; Beullens, M.; Van Eynde, A.; Bollen, M. A substrate-trapping strategy for protein phosphatase PP1 holoenzymes using hypoactive subunit fusions. *J. Biol. Chem.* **2018**, *293*, 15152–15162.
- (5) Chatterjee, J.; Beullens, M.; Sukackaite, R.; Qian, J.; Lesage, B.; Hart, D. J.; Bollen, M.; Köhn, M. Development of a peptide that selectively activates protein phosphatase-1 in living cells. *Angew. Chem., Int. Ed.* **2012**, *51*, 10054–10059.
- (6) Wang, Y.; Hoermann, B.; Pavic, K.; Trebacz, M.; Rios, P.; Köhn, M. Interrogating PP1 Activity in the MAPK Pathway with Optimized PP1-Disrupting Peptides. *ChemBioChem* **2019**, *20*, 66–71.
- (7) Reither, G.; Chatterjee, J.; Beullens, M.; Bollen, M.; Schultz, C.; Köhn, M. Chemical activators of protein phosphatase-1 induce calcium release inside intact cells. *Chem. Biol.* **2013**, *20*, 1179–1186.
- (8) Fischer, T. H.; Eiringhaus, J.; Dybkova, N.; Saadatmand, A.; Pabel, S.; Weber, S.; Wang, Y.; Köhn, M.; Tirilomis, T.; Ljubojevic, S.; Renner, A.; Gummert, J.; Maier, L. S.; Hasenfuß, G.; El-Armouche, A.; Sossalla, S. Activation of protein phosphatase 1 by a selective phosphatase disrupting peptide reduces sarcoplasmic reticulum Ca<sup>2+</sup> leak in human heart failure. *Eur. J. Heart Failure* **2018**, *20*, 1673–1685.
- (9) Eiringhaus, J.; Herting, J.; Schatter, F.; Nikolaev, V. O.; Sprenger, J.; Wang, Y.; Köhn, M.; Zabel, M.; El-Armouche, A.; Hasenfuss, G.; Sossalla, S.; Fischer, T. H. Protein kinase/phosphatase balance mediates the effects of increased late sodium current on ventricular calcium cycling. *Basic Res. Cardiol.* **2019**, *114*, 13.
- (10) Adams, S. R.; Tsien, R. Y. Controlling cell chemistry with caged compounds. *Annu. Rev. Physiol.* **1993**, *55*, 755–784.
- (11) Brieke, C.; Rohrbach, F.; Gottschalk, A.; Mayer, G.; Heckel, A. Light-controlled tools. *Angew. Chem., Int. Ed.* **2012**, *51*, 8446–8476.
- (12) Ankenbruck, N.; Courtney, T.; Naro, Y.; Deiters, A. Optochemical Control of Biological Processes in Cells and Animals. *Angew. Chem., Int. Ed.* **2018**, *57*, 2768–2798.
- (13) Bardhan, A.; Deiters, A. Development of photolabile protecting groups and their application to the optochemical control of cell signaling. *Curr. Opin. Struct. Biol.* **2019**, *57*, 164–175.
- (14) Dai, Z.; Dulyaninova, N. G.; Kumar, S.; Bresnick, A. R.; Lawrence, D. S. Visual Snapshot of Intracellular Kinase Activity at Onset of Mitosis. *Chem. Biol.* **2007**, *14* (11), 1254–1260.
- (15) Veldhuyzen, W. F.; Nguyen, Q.; McMaster, G.; Lawrence, D. S. A light-activated probe of intracellular protein kinase activity. *J. Am. Chem. Soc.* **2003**, *125*, 13358–13359.
- (16) Goubko, C. A.; Majumdar, S.; Basak, A.; Cao, X. Hydrogel cell patterning incorporating photocaged RGDS peptides. *Biomed. Microdevices* **2010**, *12*, 555–568.
- (17) Xie, X.; Yang, Y.; Yang, Y.; Zhang, H.; Li, Y.; Mei, X. A photo-responsive peptide- and asparagine-glycine-arginine (NGR) peptide-mediated liposomal delivery system. *Drug Delivery* **2016**, *23* (7), 2445–2456.
- (18) Yamashiro, D.; Li, C. H. Adrenocorticotropins. 44. Total synthesis of the human hormone by the solid-phase method. *J. Am. Chem. Soc.* **1973**, *95*, 1310–1315.
- (19) Tatsu, Y.; Shigeri, Y.; Sogabe, S.; Yumoto, N.; Yoshikawa, S. Solid-phase synthesis of caged peptides using tyrosine modified with a photocleavable protecting group: application to the synthesis of caged neuropeptide Y. *Biochem. Biophys. Res. Commun.* **1996**, *227*, 688–693.
- (20) Liu, X.; Malins, L. R.; Roche, M.; Sterjovski, J.; Duncan, R.; Garcia, M. L.; Barnes, N. C.; Anderson, D. A.; Stone, M. J.; Gorry, P. R.; Payne, R. J. Site-selective solid-phase synthesis of a CCR5 sulfopeptide library to interrogate HIV binding and entry. *ACS Chem. Biol.* **2014**, *9*, 2074–2081.
- (21) Vagnarelli, P.; Ribeiro, S.; Sennels, L.; Sanchez-Pulido, L.; de Lima Alves, F.; Verheyen, T.; Kelly, D. A.; Ponting, C. P.; Rappsilber, J.; Earnshaw, W. C. Repo-Man coordinates chromosomal reorganization with nuclear envelope reassembly during mitotic exit. *Dev. Cell* **2011**, *21*, 328–342.
- (22) Qian, J.; Lesage, B.; Beullens, M.; Van Eynde, A.; Bollen, M. PP1/Repo-man dephosphorylates mitotic histone H3 at T3 and regulates chromosomal aurora B targeting. *Curr. Biol.* **2011**, *21*, 766–773.
- (23) Nilsson, J. Protein phosphatases in the regulation of mitosis. *J. Cell Biol.* **2019**, *218*, 395–409.
- (24) Moura, M.; Conde, C. Phosphatases in Mitosis: Roles and Regulation. *Biomolecules* **2019**, *9*, 55.
- (25) Terentyev, D.; Hamilton, S. J. Regulation of the sarcoplasmic reticulum Ca<sup>2+</sup> release by serine-threonine phosphatases in the heart. *J. Mol. Cell. Cardiol.* **2016**, *101*, 156–164.